**Table S1. Direct hydrogen bonds and ion pairs between CdiA-CT/CdiI toxin/immunity proteins.**

| | CdiA-CT toxin | CdiI immunity | Distance (Å) |
|---|---|---|---|
| **EC869$_{o11}$** | | | |
| Main-Side | Lys242 NZ | Ile137 O | 2.73 |
| | Arg249 NH2 | Phe75 O | 2.72 |
| | Glu250 O | Thr31 OG1 | 3.65 |
| Side-Side | Asp187 OD2 | Arg71 NE | 2.82 |
| | Lys242 NZ | Asn138 OD1 | 3.90 |
| | Tyr244 OH | Lys128 NZ | 3.99 |
| | Glu243 OE1 | Arg122 NE | 3.15 |
| | Glu243 OE2 | Arg122 NE | 3.70 |
| | Glu243 OE2 | Lys109 NZ | 3.33 |
| | Glu243 OE2 | Arg122 NH2 | 3.10 |
| | Ser247 OG | Glu130 OE1 | 3.36 |
| | Glu250 OE1 | Arg122 NH2 | 3.18 |
| | Glu250 OE2 | Arg122 NH2 | 3.39 |
| | Glu250 OE2 | Thr31 OG1 | 3.82 |
| | Glu250 OE2 | Asn12 ND2 | 3.08 |
| | Glu250 OE1 | Lys109 NZ | 3.12 |
| **YPIII** | | | |
| Main-Side | Thr250 O | Asn30 ND2 | 3.89 |
| | Lys243 NZ | Pro133 O | 2.85 |
| | Glu242 OE2 | Leu147 N | 3.72 |
| | Ala203 O | Arg28 NE | 2.92 |
| | Thr204 O | Arg28 NE | 3.43 |
| | Thr204 O | Arg28 NH2 | 3.43 |
| | Met255 O | Arg28 NH1 | 2.79 |
| Side-Side | Lys243 NZ | Ser132 OG | 2.55 |
| | Lys195 NZ | Glu137 OE1 | 2.68 |
| | Lys195 NZ | Glu137 OE2 | 3.01 |
| | Arg202 NH1 | Ser29 OG | 2.99 |
| | Lys243 NZ | Asp121 OD2 | 3.05 |
| | Asp201 OD1 | Arg69 NH1 | 2.71 |
| | Asp201 OD2 | Arg69 NH2 | 3.09 |

**Table S2. Bacterial strains and plasmids**

| ***Strain or plasmid*** | ***Description***[a] | ***Reference or source*** |
|---|---|---|
| ***Strains*** | | |
| BL21-Gold(DE3) | *E. coli* B $F^-$ *ompT hsdS*($r_B^-$ $m_B^-$) *dcm*$^+$ *gal* λ(DE3) *endA*, $Tet^R$ | Agilent |
| EPI100 | $F^-$ *mcrA* Δ*(mrr-hsdRMS-mcrBC) φ80dlacZ*Δ*M15* Δ*lacXcZ*Δ*M15* Δ*lacX recA1 endA1 araD139* Δ*(ara, leu)7697 galU galK* $\lambda^-$ *rpsL nupG*, $Str^R$ | Epicentre |
| EPI100 *pir*$^+$ | $F^-$ *mcrA* Δ*(mrr-hsdRMS-mcrBC) φ80dlacZ*Δ*M15* Δ*lacXcZ*Δ*M15* Δ*lacX recA1 endA1 araD139* Δ*(ara, leu)7697 galU galK* $\lambda^-$ *rpsL nupG pir*$^+$*(DHFR)*, $Str^R$ $Tp^R$ | Epicentre |
| X90 | F´ *lacI*$^q$ *lac´ pro´/ara* Δ*(lac-pro) nal1 argE*(amb) *rif*$^r$ *thi-1*, $Rif^R$ | [1] |
| DY378 | W3110 λ*cI857* Δ*(cro-bioA*) | [2] |
| DA28100 | *galK*::sYFP2opt-cat | Dan Andersson |
| CH2016 | X90 (DE3) Δ*rna* Δ*slyD::kan*, $Rif^R$ $Kan^R$ | [3] |
| CH2550 | EPI1100 *galK*::sYFP2opt-kan | This study |
| CH2567 | MC4100 *mKate::cam* $Str^R$ $Cm^R$ | This study |
| CH8251 | MC4100 *rif*$^r$, $Str^R$ $Rif^R$ | [4] |
| | | |
| ***Plasmids*** | | |
| pTrc99a | IPTG-inducible expression plasmid, $Amp^R$ | GE Healthcare |
| pTrc99KX | Derivative of pTrc99A that contains KpnI restriction site immediately downstream of the ribosome-binding site, $Amp^R$ | [5] |
| pCH450 | pACYC184 derivative with *E. coli araBAD* promoter for arabinose-inducible expression, $Tet^R$ | [6] |
| pSIM6 | Heat-inducible expression of the phage λ Red recombinase proteins, $Amp^R$ | [7] |
| pET21S | pET21d derivative with SpeI restriction site for in-frame fusion to $His_6$ coding sequences, $Amp^R$ | [8] |
| pDE1013 | pEndy1013-mKate2::cat | [9] |
| pNAK | pBluescript derivative with FRT-flanked kanamycin-resistance cassette, $Amp^R$ $Kan^R$ | This study |
| pDAL878 | Constitutive expression of *cdiA*$^{EC93}$*-(*Δ*CT)*, in which the toxin-encoding sequence has been deleted, $Cm^R$ | [8] |
| pCH10164 | Constitutive expression of chimeric *cdiA*$^{EC93}$*-CT(D198A)*$_{o11}^{EC869}$ and *cdiI* $_{o11}^{EC869}$. The Asp198Ala mutation inactivates the DNase domain. $Cm^R$ | [4] |
| pCH848 | pTrc99KX::*cdiI*$^{YPIII}$, $Amp^R$ | This study |

| | | |
|---|---|---|
| pCH2409 | Constitutive expression of chimeric *cdiA*$^{EC93}$-*CT*$^{YPIII}$ and *cdiI*$^{YPIII}$ genes, Cm$^R$ | This study |
| pCH2500 | pNAK::*galM´*, Amp$^R$ Kan$^R$ | This study |
| pCH2503 | pNAK::*galT´-yfp-galM´*, Amp$^R$ Kan$^R$ | This study |
| pCH9305 | Constitutive expression of chimeric *cdiA*$^{EC93}$-*CT*$_{o11}$$^{EC869}$ and *cdiI*$_{o11}$$^{EC869}$ genes, Cm$^R$ | [4] |
| pCH9315 | pTrc99A::*cdiI*$_{o11}$$^{EC869}$, Amp$^R$ | [4] |
| pCH9938 | pUC57::NEILACOT_05636 encoding CdiI$^{Nlact}$ from *Neisseria lactamica* ATCC 23970, Amp$^R$ | This study |
| pCH9940 | pUC57::Ykris_10749 encoding CdiI$^{Ykris}$ from *Yersinia pseudotuberculosis* ATCC 33638, Amp$^R$ | This study |
| pCH10101 | pCH450::NEILACOT_05636, Tet$^R$ | This study |
| pCH10103 | pTrc99KX::Ykris_10749, Amp$^R$ | This study |
| pCH10163 | Cosmid pCdiA-CT/*pheS** that carries a *kan-pheS** cassette in place of the *E. coli* EC93 *cdiA-CT/cdiI* coding sequence. Used for allelic exchange and counter-selection. Cm$^R$ Kan$^R$ | [4] |
| pCH10170 | pET21-derivative that expresses CdiI$^{Ykris}$-His$_6$ from *Y. kristensenii* ATCC 33638, Amp$^R$ | This study |
| pCH10172 | pET21-derivative that expresses CdiI$^{Nlact}$-His$_6$ *N. lactamica* ATCC 23970, Amp$^R$ | This study |
| pCH10175 | pET21-derivative that expresses CdiA-CT(D198A)$_{o11}$$^{EC869}$ containing the β4/β5 hairpin from CdiA-CT$^{Ykris}$, Amp$^R$ | This study |
| pCH10365 | pET21-derivative that expresses CdiA-CT(D198A)$_{o11}$$^{EC869}$ containing the β4/β5 hairpin from CdiA-CT$^{Nlact}$, Amp$^R$ | This study |
| pCH10367 | pET21-derivative that expresses CdiI$^{YPIII}$-His$_6$ from from *Y. pseudotuberculosis* YPIII, Amp$^R$ | This study |
| pCH10369 | pET21-derivative that expresses CdiA-CT$_{o11}$$^{EC869/Δβ4β5}$ lacking the β4/β5 hairpin, Amp$^R$ | This study |
| pCH10407 | pET21-derivative that expresses CdiA-CT/CdiI$_{o11}$$^{EC869}$-His$_6$ complex from *E. coli* EC869, Amp$^R$ | [4] |
| pCH10413 | pET21-derivative that expresses CdiA-CT/CdiI$^{YPIII}$-His$_6$ complex from *Y. pseudotuberculosis* YPIII, Amp$^R$ | This study |

[a]Abbreviations: Amp$^R$, ampicillin-resistant; Cm$^R$, chloramphenicol-resistant; Kan$^R$, kanamycin-resistance; Rif$^R$, rifampicin-resistant; Tet$^R$, tetracycline-resistant; Tp$^R$, trimethoprim-resistant

**Table S3**. Oligonucleotides used in this study.

| Oligonucleotide | Sequence | Reference |
|---|---|---|
| Kan-1 (CH106) | 5′ - TGT GTA GGC TGG AGC TGC TTC | [10] |
| Kan-2 (CH107) | 5′ - CAT ATG AAT ATC CTC CTT AGT TCC | [10] |
| galM-Bam-for (CH3789) | 5′ - CGC GGA TCC CGG AAG AGC TGG | This study |
| galM-Sac-rev (CH3790) | 5′ - TCT GAG CTC AGG GCA AAC AGC ACC | This study |
| galT-Kpn-for (CH3787) | 5′ - CAC GGT ACC ATT TGG GCA AAT AGC TTC C | This study |
| yfp-Eco-rev (CH3788) | 5′ - CT GAA TTC GCG GCC GCT TCT AGA | This study |
| YPK0575-Kpn-for (CH2447) | 5′ - TTT GGT ACC ATG GTA GAG AAT AAT TAT CTA AAC TCC | This study |
| YPK0576-Xho-rev (CH2448) | 5′ - TTC CTC GAG ACC TTT ACA GCG ACT CAA TGC CAG | This study |
| YPK0576-Kpn-for (CH2449) | 5′ - TGA GGT ACC ATG AAC GAT ATA GTA AAA AG | This study |
| YPK0576-Xho-rev2 (CH2790) | 5′ - TTT CTC GAG TTA ACC TTT ACA GCG | This study |
| Nlact-cdiI-Spe-rev (CH2345) | 5′ - AAA ACT AGT CTT ACA ATA ACT TAG | This study |
| Ykris-cdiI-Spe-rev (CH2346) | 5′ - AAA ACT AGT GCC TTT ACA GCG GC | This study |
| Trc-seq2 (CH823) | 5′ - GTT CTG GCA AAT ATT CTG AAA TGA GC | This study |
| ara seq (CH943) | 5′ - GAT TAG CGG ATC CTA CCT GAC GCT TTT TAT CGC | This study |
| β-deletion-for1 | 5′ - GCC CAA TGG GCA CAA ACC AGT CTC TGA CCT TCG AT | This study |
| β-deletion-rev1 | 5′ - GCG GAT CCG CTT TTA AAC TTA GCC GCA GCA TCG ATG | This study |
| β-deletion-for2 | 5′ - GCG GAT CCG GCA CTT CAT CAA TGA TCT CTA ACA GGG | This study |
| β-deletion-rev2 | 5′ - GCC TCG AGA CTA GTA CCT TTG CAG CGA CTC AAG | This study |
| EC869-CT-Nco | 5′ - ATT CCA TGG GCA CAA ACC AGT CTC TGA CCT TCG | [4] |
| EC869-cdiI-Spe | 5′ - TCT ACT AGT ACC TTT GCA GCG ACT CAA GGC CAG | [4] |
| EC869-Nlact(beta)-for | 5′ - AAA ACT TAC TCT CTT TCT GGT GTT GAG TTA ACT TCA TCA ATG ATC TC | This study |

| | | |
|---|---|---|
| (CH2341) | | |
| EC869-Nlact(beta)-rev (CH2342) | 5′ - CTC AAC ACC AGA AAG AGA GTA AGT TTT AAA CTT AGC CGC AGC ATC G | This study |
| EC869-Ykris(beta)-for (CH2343) | 5′ - CAT ACA CAT ACT CTT TCA GGC GAA CAG TTA ACT TCA TCA ATG ATC TC | This study |
| EC869-Ykris(beta)-rev (CH2344) | 5′ - CTG TTC GCC TGA AAG AGT ATG TGT ATG AAA CTT AGC CGC AGC ATC G | This study |
| DL1527 (CDI204) | 5′ - GAA CAT CCT GGC ATG AGC G | [4] |
| EC869o11-G173-rev (CH3640) | 5′ - CCC AAC ATA ATC CTC CCA CGG CAT ACC | This study |
| EC869o11-G173-for (CH3641) | 5′ - GGT ATG CCG TGG GAG GAT TAT GTT GGG | This study |
| EC93-YPIII-chim-rev (CH2689) | 5′ - GGT CTG GTG TCT AAC CTT TGG GTT AAC CTT TAC AGC GAC TCA ATG C | This study |
| EC93-YPIII-down-for (CH2690) | 5′ - GCA TTG AGT CGC TGT AAA GGT TAA CCC AAA GGT TAG ACA CCA GAC C | This study |
| DL2368 (CDI205) | 5′ - GTT GGT AGT GGT GGT GCT G | [4] |

## References


1. Beckwith, J. R. & Signer, E. R. (1966). Transposition of the lac region of *Escherichia coli*. I. Inversion of the *lac* operon and transduction of *lac* by phi80. *J Mol Biol* **19**, 254-65.
2. Thomason, L., Court, D. L., Bubunenko, M., Costantino, N., Wilson, H., Datta, S. & Oppenheim, A. (2007). Recombineering: genetic engineering in bacteria using homologous recombination. *Curr Protoc Mol Biol* **Chapter 1**, Unit 1 16.
3. Garza-Sanchez, F., Janssen, B. D. & Hayes, C. S. (2006). Prolyl-tRNA(Pro) in the A-site of SecM-arrested ribosomes inhibits the recruitment of transfer-messenger RNA. *J Biol Chem* **281**, 34258-68.
4. Morse, R. P., Nikolakakis, K. C., Willett, J. L., Gerrick, E., Low, D. A., Hayes, C. S. & Goulding, C. W. (2012). Structural basis of toxicity and immunity in contact-dependent growth inhibition (CDI) systems. *Proc Natl Acad Sci U S A* **109**, 21480-5.
5. Koskiniemi, S., Garza-Sanchez, F., Sandegren, L., Webb, J. S., Braaten, B. A., Poole, S. J., Andersson, D. I., Hayes, C. S. & Low, D. A. (2014). Selection of orphan Rhs toxin expression in evolved *Salmonella enterica* serovar Typhimurium. *PLoS Genet* **10**, e1004255.
6. Hayes, C. S. & Sauer, R. T. (2003). Cleavage of the A site mRNA codon during ribosome pausing provides a mechanism for translational quality control. *Mol Cell* **12**, 903-11.
7. Datta, S., Costantino, N. & Court, D. L. (2006). A set of recombineering plasmids for gram-negative bacteria. *Gene* **379**, 109-15.
8. Poole, S. J., Diner, E. J., Aoki, S. K., Braaten, B. A., t'Kint de Roodenbeke, C., Low, D. A. & Hayes, C. S. (2011). Identification of functional toxin/immunity genes linked to contact-dependent growth inhibition (CDI) and rearrangement hotspot (Rhs) systems. *PLoS Genet* **7**, e1002217.
9. Bonnet, J., Subsoontorn, P. & Endy, D. (2012). Rewritable digital data storage in live cells via engineered control of recombination directionality. *Proc Natl Acad Sci U S A* **109**, 8884-9.
10. Hayes, C. S., Bose, B. & Sauer, R. T. (2002). Proline residues at the C terminus of nascent chains induce SsrA tagging during translation termination. *J Biol Chem* **277**, 33825-32.

**Figure legends**

**Figure S1. The macrocyclic peptide mimic of the β-hairpin from CdiA-CT$_{o11}^{EC869}$.**

**Figure S2. Comparison of CdiA-CT catalytic sites.** In both panels EC869 and YPIII carbon atoms are depicted in white and grey, respectively, and oxygen and nitrogen atoms are colored red and blue, respectively. (**A**) CdiA-CT$_{o11}^{EC869}$ active site contains a $Zn^{2+}$ ion, depicted by at purple sphere with water molecules depicted as smaller red spheres, and interacting bonds with $Zn^{2+}$ are depicted as black dotted lines. (**B**) CdiA-CT$^{YPIII}$ active site has no extra density that would create a zinc coordination sphere. Water molecules are depicted as yellow spheres.

**Figure S3**. **Alignments of CdiA-CT/CdiI$_{o11}^{EC869}$ family members.** (**A**) Alignment of DNase toxin domain homologues. Residue are numbered according to the CdiA-CT$_{o11}^{EC869}$ sequence beginning with Val1 of the VENN peptide motif. The alignment was rendered with Jalview at 30% sequence identity with progressively darker shades of purple indicating greater residue conservation. Secondary structure elements correspond to CdiA-CT$_{o11}^{EC869}$. CdiA-CT$_{o11}^{EC869}$ and CdiA-CT$^{YPIII}$ residues that form H-bonds/ion-pairs with cognate immunity proteins are shown in orange, and residues that form hydrophobic/van der Waals contacts are shown in blue. (**B**) Alignment of immunity protein homologues. Residue numbers and secondary structure elements correspond to CdiI$_{o11}^{EC869}$. Residues that interact with toxins are color coded according the scheme described for panel **A**.

**Figure S4**. **Electrostatic surfaces of CdiA-CT/CdiI$_{o11}^{EC869}$ and CdiA-CT/CdiI$^{YPIII}$ complexes.** Electrostatic surface representation of CdiI$_{o11}^{EC869}$ (**A**) and CdiI$^{YPIII}$ (**B**). Red and blue surfaces correspond to positive and negative surface potentials (respectively) and white indicates hydrophobic surfaces. Toxin β-hairpins are show in stick representation in the left panels. Right panels are rotated 180° around the y-axis with respect to the left panels and the immunity proteins are shown in cartoon representation.

**Figure S5. Target cells become filamentous after inhibition by the $CDI_{o11}^{EC869}$ and $CDI^{YKris}$ systems.** Co-culture competitions were performed using mock inhibitors or inhibitor cells deploying the $CDI_{o11}^{EC869}$ and $CDI^{YPIII}$ systems and target cells carrying an empty vector (none) or a plasmid expressing $CdiI_{o11}^{EC869}$ or $CdiI^{YPIII}$. Cell length values were measured from microscopy images taken of each competition. Each object plotted represents the length of a single cell. Black bars indicate the mean of each data set. *P* values from two-tailed unpaired t-tests are reported. ***, *P*=<0.0001.

**Figure S6**. **Superimposition of immunity protein homologues**. The $CdiI^{YPIII}$, $CdiI_{o11}^{EC869}$, $CdiI^{Ykris}$ and $CdiI^{Nmen}$ immunity proteins are depicted in cartoon representations colored in magenta, cyan, gold and gray, respectively. The structures of $CdiI^{Nmen}$ (PDB ID: 2GKP) and $CdiI^{Ykris}$ were determined in the absence of bound toxin. The location of the β-hairpin binding pocket is indicated and the extended loop (E-L) connecting α1* to α2* of $CdiI^{YPIII}$ is labeled.

**Figure S7**. **Electrostatic surface potential of toxin β-hairpin chimeras.** (**A**) Electrostatic surface representation of $CdiI_{o11}^{EC869}$ with the toxin β-hairpin in cartoon and sticks colored green (left panel). The right panel is rotated 180° around the y-axis with respect to the left panel. The immunity protein is depicted as cartoon representation and the toxin β-hairpin is rendered as an electrostatic surface representation. (**B**) and (**C**) Models of CdiA-$CT^{Nlact}$ and CdiA-$CT^{Ykris}$ β-hairpins docked onto $CdiI_{o11}^{EC869}$ immunity protein. The models are viewed in the same orientation as the right image in panel **A**. The β-hairpins are rendered as electrostatic surface representations, with red and blue representing positive and negative surface potentials (respectively) and white indicating hydrophobic surfaces.

**Figure S1**

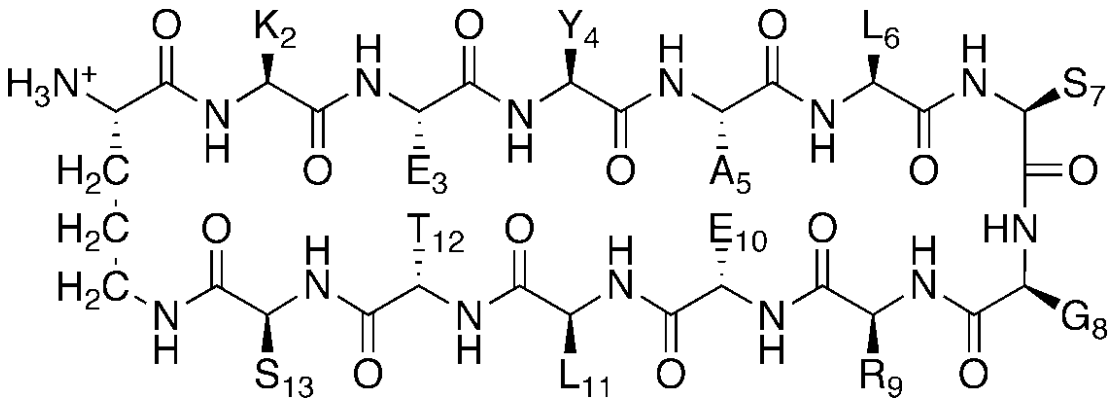

**Figure S2**

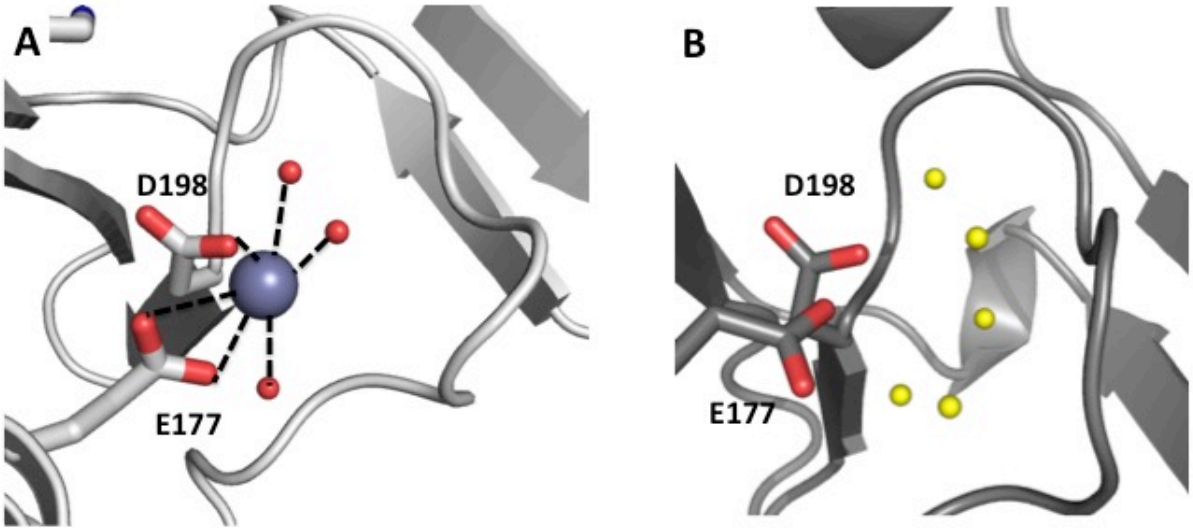

# Figure S3

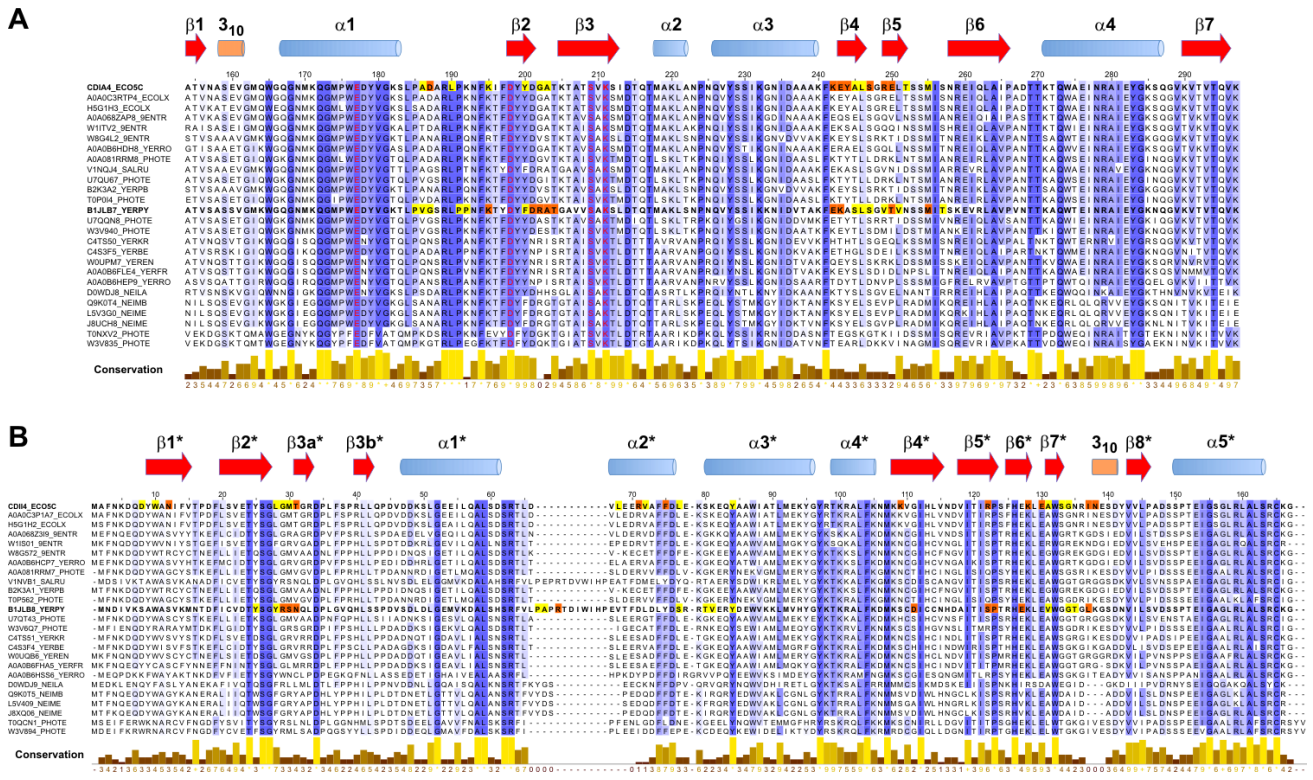
A
β1
3₁₀
α1
β2
β3
α2
α3
β4
β5
β6
α4
β7
Conservation
B
β1*
β2*
β3a*
β3b*
α1*
α2*
α3*
α4*
β4*
β5*
β6*
β7*
3₁₀
β8*
α5*
Conservation

Figure S4

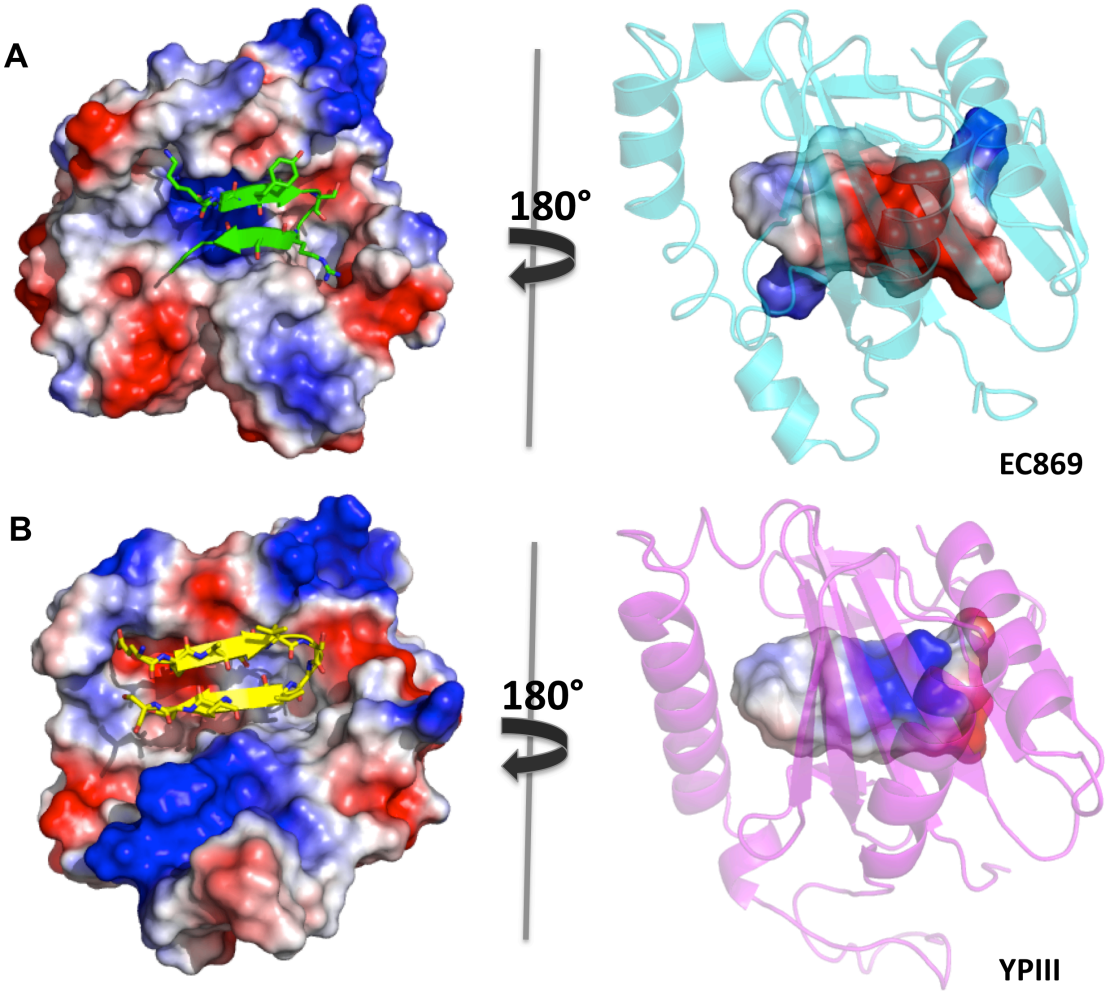

**Figure S5**

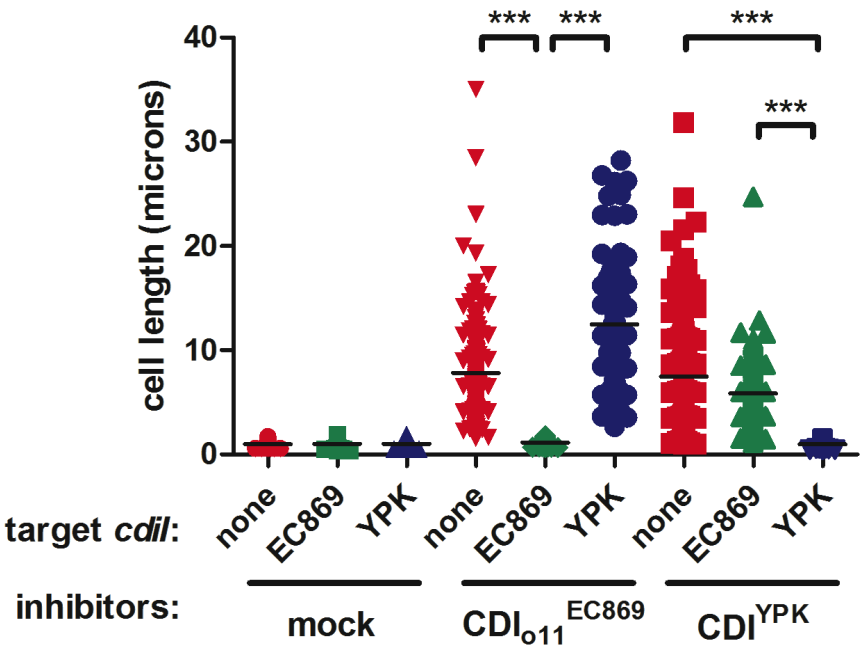
***
***
***
***
40
30
20
10
0
cell length (microns)
target cdil:
none
EC869
YPK
none
EC869
YPK
none
EC869
YPK
inhibitors:
mock
CDI o11 EC869
CDI YPK

**Figure S6**

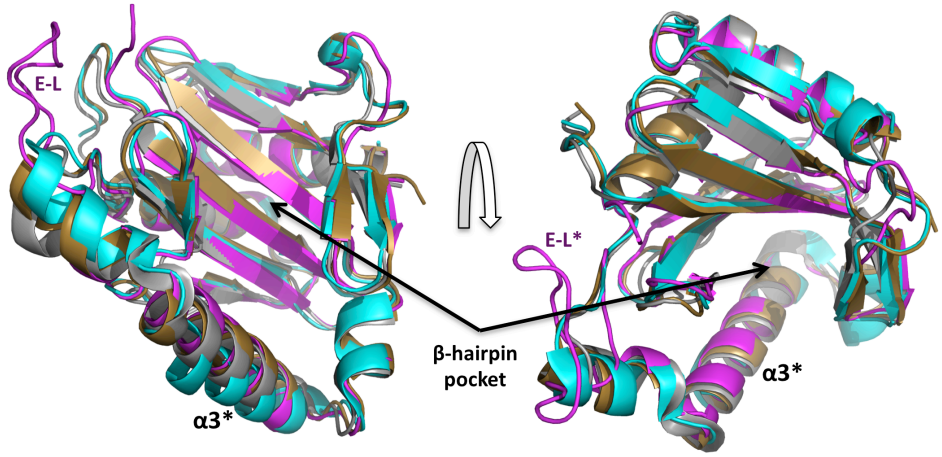

Figure S7